Real-time and low-cost sensing technique based on photonic bandgap structures

J. G. Castelló,[1,*] V. Toccafondo,[1] P. Pérez-Millán,[1] N. S. Losilla,[1] J. L. Cruz,[2] M. V. Andrés,[2] and J. García-Rupérez[1]

[1]Nanophotonics Technology Center, Universidad Politécnica de Valencia, Camino de Vera s/n, 46022 Valencia, Spain

[2]Departamento de Física Aplicada y Electromagnetismo, Universidad de Valencia, Dr. Moliner 50, Burjassot 46100, Valencia, Spain

*Corresponding author: jagarcas@ntc.upv.es

Received May 26, 2011; revised June 13, 2011; accepted June 13, 2011; posted June 14, 2011 (Doc. ID 148157); published July 14, 2011

A technique for the development of low-cost and high-sensitivity photonic biosensing devices is proposed and experimentally demonstrated. In this technique, a photonic bandgap structure is used as transducer, but its readout is performed by simply using a broadband source, an optical filter, and a power meter, without the need of obtaining the transmission spectrum of the structure; thus, a really low-cost system and real-time results are achieved. Experimental results show that it is possible to detect very low refractive index variations, achieving a detection limit below 2×10^{-6} refractive index units using this low-cost measuring technique.

OCIS codes: 130.6010, 130.5296.

Having fast, efficient, and reliable sensing devices is essential in many fields, such as medical diagnostics, food safety control, environmental control, and drug detection [1]. In recent years, photonic technology has attracted a lot of interest for the development of these sensing devices for the detection and quantification of substances and analytes such as gases, proteins, hormones, bacteria, and DNA. Although more mature photonic sensing technologies, such as those based on surface plasmon resonances [2] or fiber Bragg gratings [3], even became commercially available some years ago, devices based on integrated planar photonic structures are envisaged as a highly promising alternative for future lab-on-a-chip (LoC) devices. This is due to several advantages they present compared to previously mentioned sensing technologies, such as compactness, the possibility for multianalyte detection, high sensitivity, high interaction between optical field and target analytes, shorter detection time, label-free detection, and the requirement of very low volumes to perform the sensing. Moreover, the possibility of using mass manufacturing complementary metal-oxide semiconductor techniques allows VLSI of the final devices, which results in a drastic reduction of their cost.

Planar photonic sensing devices, which have been most used in the past few years, base their detection on the direct measurement of the shift of the structure's spectral response, as it occurs for ring resonators [4–6] or photonic crystals [7–10]. Therefore, these systems require the use of either a tunable laser source or an optical spectrum analyzer (OSA) to perform the readout of the device, making the total cost of the system significant. Moreover, sweeping times of the order of several seconds up to minutes are needed to acquire each spectrum, preventing an instantaneous observation of the interactions of the target analyte with the sensor. Other photonic structures, such as directional couplers [11] or Mach–Zehnder interferometers (MZIs) [12], which do not require tunable elements in the readout system and would thus allow a reduction in the final cost of the system, have also been proposed. However, compared to ring resonators or photonic crystals, these structures require much larger lengths in order to have enough interaction between the optical field and the target analyte, so that their integration level is limited (note that more compact designs for MZI-based sensors have been proposed [13]).

In this Letter, we propose and experimentally demonstrate a new technique for the development of real-time and low-cost integrated photonic sensing devices. The sensing technique is based on using photonic bandgap (PBG) structures to perform the detection, but the PBG shift is indirectly determined by using a filtered broadband optical source as excitation instead of a tunable laser and a power meter at the output, thus significantly simplifying the system and reducing its cost.

The working principle underlying the proposed sensing technique is described in Fig. 1. An input optical signal with a given bandwidth and a constant power is used as excitation for the photonic sensing structure, which consists of a periodic dielectric structure with a PBG edge located within the source wavelength range (for the case shown in Fig. 1, the upper edge of the PBG is used for the sensing). The PBG filters the optical source, and the overlap of both spectra can be directly measured at

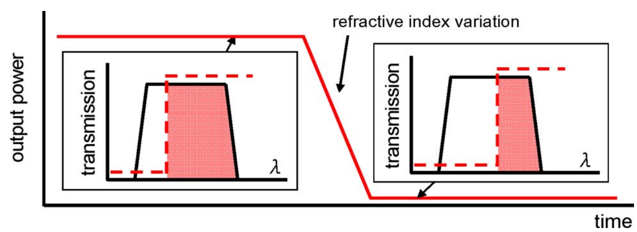

Fig. 1. (Color online) Output power evolution using the proposed sensing technique. In the initial state, the source spectrum (black solid line) is filtered by the PBG of the sensing structure (red dashed line) and only a certain amount of power is transmitted (shaded area). When a refractive index variation occurs, the PBG shifts, and the amount of input power filtered changes (decreases in this case).

the output using a simple power meter. When a variation of the refractive index (RI) of the surrounding medium occurs, it induces a shift in the spectral response of the photonic sensing structure. This is translated into a shift in the position of the PBG edge, and thus to a change in the optical power measured at the output, as can be seen in Fig. 1, where an increase in the RI of the surrounding medium occurs. The spectral shift can be induced both by the bulk RI variation of the surrounding medium or by the binding of a target analyte, such as a protein or DNA strand, on the sensor surface. This power variation is directly used to perform the sensing, without the need to obtain the transmission spectrum of the structure using expensive tunable elements. Moreover, since the output power can be continuously monitored (several power values per second can be measured), a real-time sensing is performed, which allows an instantaneous observation of the interactions taking place in the sensing structure.

The initial alignment between the source and the sensor will determine the sensitivity and the linearity of the device, as shown in Fig. 2. A high initial overlapping between the source and the sensor leads to a linear response of the sensor, although a lower sensitivity is obtained. On the other hand, as the initial overlapping is reduced, the sensitivity increases, but a more nonlinear behavior is observed. However, a proper modeling and calibration of the sensor response will allow working in the nonlinear regime, with a significant increase in the sensor sensitivity.

For the experimental demonstration of this technique, we have used a corrugated waveguide [14,15] fabricated in a silicon-on-insulator (SOI) wafer with a 220 nm-thick silicon layer on a 2 μm-thick buried oxide layer, which is shown in Fig. 3. The fabrication of the structures has been performed through the ePIXfab service at CEA-LETI, France. 450 nm-wide single-mode waveguides are used to access the corrugated waveguide, which is created by simply introducing transversal straight elements in the single-mode waveguide. The parameters of the corrugated waveguide have been selected to achieve a PBG around 1550 nm for TE-polarized light, yielding a lattice constant (a) of 380 nm, an element width (w_i) of 160 nm,

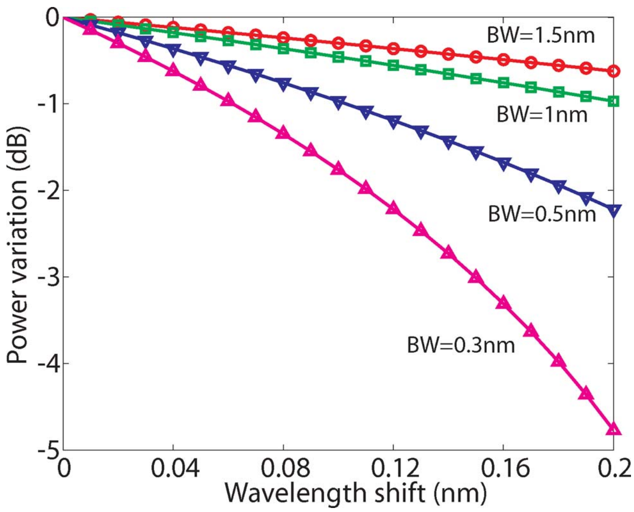

Fig. 2. (Color online) Power variation versus wavelength shift for different initial alignments between the source and the sensor. BW, initial overlapping bandwidth.

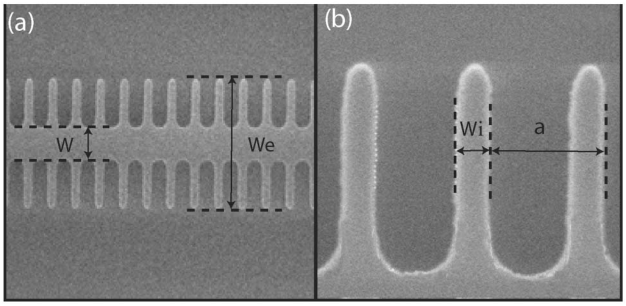

Fig. 3. (a) Scanning electron microscope image of the SOI corrugated waveguide used for sensing, (b) closeup view of the transversal elements.

and an element length (w_e) of 2 μm, while the corrugated waveguide length was set to 38 μm (101 transversal elements). Finally, the single-mode access waveguides are tapered to a width of 2.5 μm to reduce transmission losses. The whole device is accessed through TE-optimized grating couplers.

On top of the SOI photonic device, a perpendicular microfluidic channel is created for an optimal delivering of the target substance to the sensing structure. A 50 μm-high and 400 μm-wide channel with two 1 mm-wide access reservoirs has been fabricated in SU8 polymer using UV lithography in our in house facilities. The channel was sealed with a flat lid of polydimethylsiloxane with two access ports positioned above the reservoirs and connected to silicone tubing. For sample delivery, a pump working in withdraw mode is used (with a flow rate of 20 μl/ min) in order to absorb liquids from a vessel and drive them over the sensing structure. This pumping configuration eases the change of the target sample to be delivered.

The normalized response near the upper PBG edge of the corrugated waveguide used in the experiments with a deionized water (DIW) uppercladding is depicted in Fig. 4.

In order to obtain a bandwidth-limited optical excitation, as required for the proposed sensing technique, the light from a low-cost broadband superluminescent diode

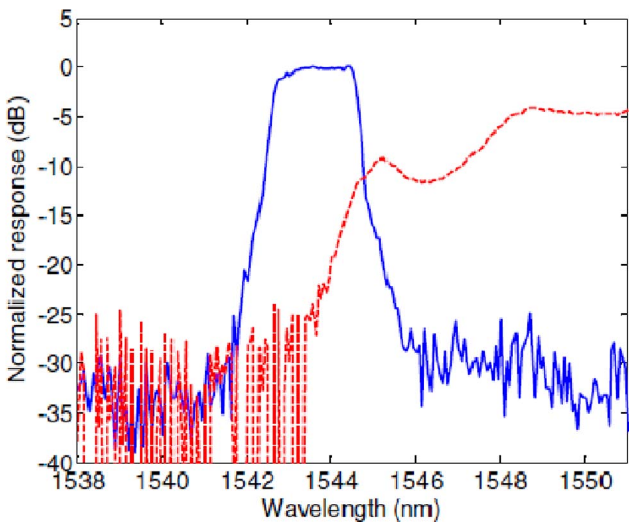

Fig. 4. (Color online) Normalized transmission spectra of the corrugated waveguide (dashed red line) and CFBG-filtered optical source (solid blue line).

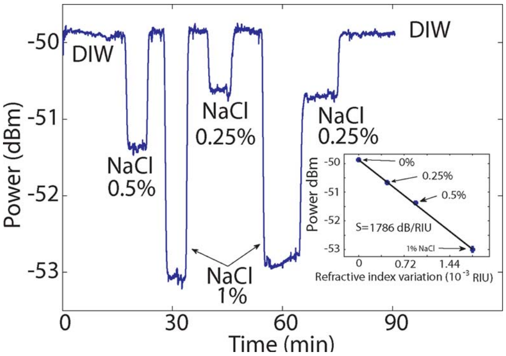

Fig. 5. (Color online) Time evolution of the output power during the flow of NaCl dilutions with different concentrations. The inset shows the sensitivity curve.

is filtered using a chirped fiber Bragg grating (CFBG) and a circulator to obtain a narrower emission spectrum of approximately 2 nm bandwidth, matching the PBG edge position of the corrugated waveguide, as can be seen in Fig. 4. The CFBG has been fabricated by UV exposure through a uniform phase mask and a proper combination of continuous fiber stretching and UV scanning movements [16]. The CFBG has a length of 50 mm and a reflectance of 95%. The filtered source is then TE-polarized and coupled to the corrugated waveguide through the input grating coupler. The output light is collected with a fiber, and a power meter is used to continuously measure the output power (in this case, we have used an integration time of 300 ms).

To perform the RI sensing experiments, we have used several NaCl dilutions in DIW with concentrations ranging from 0.25% to 1% in mass. Figure 5 shows the temporal evolution of the output power when switching among the different NaCl–DIW dilutions. It can be seen that an output power reduction occurs as the NaCl concentration increases, due to the increase of the RI of the surrounding medium, which leads to a red shift of the PBG edge position. The variation of the RI of an NaCl–DIW dilution at room temperature is $\Delta n_{\mathrm{NaCl:DIW}} = 0.00175\,\mathrm{RIU}/\%$ (refractive index units) for NaCl concentrations below 10% [17]. Note that this variation is given in [17] for a wavelength of 589 nm, but we have confirmed through a linear approximation and Cauchy dispersion coefficients that it is also valid at a wavelength of 1550 nm. From this RI variation, a significant sensitivity value of 1786 dB/RIU is obtained, as shown in the inset of Fig. 5. We can also observe a good linearity in the power variation, which indicates a proper initial alignment between the source and the sensor.

We have measured a standard deviation of the output power on the order of $\sigma \approx 0.01$ dBm. Using this value as the noise level, a detection limit of 5.6×10^{-6} RIU has been calculated. However, the detection limit can be further reduced by simply performing a temporal averaging of the raw power values obtained. A detection limit below 2×10^{-6} RIU is obtained when a 100-point temporal averaging is performed.

Finally, we have measured the wavelength sensitivity of the corrugated waveguide used as sensor. We have obtained a high-sensitivity value of the order of 150 nm/RIU. However, because of the difficulty of accurately determining the position of the band edge, a detection limit of the order of 10^{-5} RIU is estimated, 1 order of magnitude worse than the value obtained using the proposed power-based sensing technique.

In summary, we have experimentally demonstrated a new sensing technique based on the use of PBG structures, which can be employed to detect very small refractive index variations in real time and using low-cost equipment consisting solely of a broadband source and a power meter, without the necessity of a tunable laser or an OSA. Through refractive index measurements, we have estimated detection limit values below 2×10^{-6} RIU using a sensing structure with a surface of only $76\,\mu\mathrm{m}^2$. This technique is clearly promising for future sensing applications such as detection of proteins or DNA strands for future LoC, where very small spectral shifts need to be detected and quantified.

This work was funded by the Spanish Ministerio de Ciencia e Innovación (MICINN) under contracts TEC2008-06333, JCI-009-5805, and TEC2008-05490. Support by the Universidad Politécnica de Valencia through program PAID-06-09 and the Conselleria d'Educació through program GV-2010-031 is acknowledged.

References

1. X. D. Fan, I. M. White, S. I. Shopova, H. Zhu, J. D. Suter, and Y. Sun, Anal. Chim. Acta **620**, 8 (2008).
2. J. Homola, S. S. Yee, and G. Gauglitz, Sens. Actuators B **54**, 3 (1999).
3. A. D. Kersey, M. A. Davis, H. J. Patrick, M. LeBlanc, K. P. Koo, C. G. Askins, M. A. Putnam, and E. J. Friebele, J. Lightwave Technol. **15**, 1442 (1997).
4. K. De Vos, I. Bartolozzi, E. Schacht, P. Bienstman, and R. Baets, Opt. Express **15**, 7610 (2007).
5. M. Iqbal, M. A. Gleeson, B. Spaugh, F. Tybor, W. G. Gunn, M. Hochberg, T. Baehr-Jones, R. C. Bailey, and L. C. Gunn, IEEE J. Sel. Top. Quantum Electron. **16**, 654 (2010).
6. D.-X. Xu, M. Vachon, A. Densmore, R. Ma, A. Delâge, S. Janz, J. Lapointe, Y. Li, G. Lopinski, D. Zhang, Q. Y. Liu, P. Cheben, and J. H. Schmid, Opt. Lett. **35**, 2771 (2010)
7. N. Skivesen, A. Têtu, M. Kristensen, J. Kjems, L. H. Frandsen, and P. I. Borel, Opt. Express **15**, 3169 (2007).
8. M. R. Lee and P. M. Fauchet, Opt. Lett. **32**, 3284 (2007).
9. J. García-Rupérez, V. Toccafondo, M. Bañuls, J. Castelló, A. Griol, S. Peransi-Llopis, and Á. Maquieira, Opt. Express **18**, 24276 (2010).
10. V. Toccafondo, J. García-Rupérez, M. J. Bañuls, A. Griol, J. G. Castelló, S. Peransi-Llopis, and A. Maquieira, Opt. Lett. **35**, 3673 (2010).
11. B. J. Luff, R. D. Harris, J. S. Wilkinson, R. Wilson, and D. J. Schiffrin, Opt. Lett. **21**, 618 (1996).
12. B. Sepúlveda, J. S. Río, M. Moreno, F. J. Blanco, K. Mayora, C. Domínguez, and L. M. Lechuga, J. Opt. A **8**, S561 (2006).
13. A. Densmore, M. Vachon, D.-X. Xu, S. Janz, R. Ma, Y.-H. Li, G. Lopinski, A. Delâge, J. Lapointe, C. C. Luebbert, Q. Y. Liu, P. Cheben, and J. H. Schmid, Opt. Lett. **34**, 3598 (2009).
14. M. L. Povinelli, S. G. Johnson, and J. D. Joannopoulos, Opt. Express **13**, 7145 (2005).
15. J. García, P. Sanchis, A. Martínez, and J. Martí, Opt. Express **16**, 3146 (2008).
16. P. Pérez-Millán, S. Torres-Peiró, J. L. Cruz, and M. V. Andrés, Opt. Fiber Technol. **14**, 49 (2008).
17. D. R. Lide, *Handbook of Chemistry and Physics* (CRC Press, 2008).